VARIATIONS OF INTERSTELLAR ULTRA-VIOLET ABSORPTION*

SYUZO ISOBE
Tokyo Astronomical Observatory, University of Tokyo, Tokyo, Japan

Abstract. It is shown that mixtures of graphite core-ice mantle grains with large and small mean size and graphite grains provide good fits to the observed interstellar extinction curve.

Since the existence of interstellar absorption was found in 1930 by Trumpler (1930), many types of dust grains have been proposed to explain the absorption. However, as the observed wavelengths were very limited before 1965, almost any shape of reddening curve could be fitted to the observed ones by using any type of grains, if the size distribution of grains was adjusted in proper ways. Since 1965, the observed wavelengths have been extended to longer and shorter wavelengths. And in these infra-red and ultra-violet wavelengths, various types of interstellar reddening curves and circumstellar infra-red emission curves have been observed.

Stecher (1965) observed several stars at wavelengths extended to $1/\lambda \simeq 8.3\ \mu^{-1}$ and pointed out the existence of interstellar absorption bands at $1/\lambda \simeq 4.4\ \mu^{-1}$. It was already pointed out by Greenberg at this time and subsequently (Greenberg, 1966, 1967, 1968, 1969) that no model of interstellar grains which included dielectric materials with 'realistic' indices of refraction in the far ultraviolet could be used to represent the continued rise of the interstellar extinction in the far ultraviolet. All the models which presume to match the far ultraviolet extinction suffer from this defect. Carruthers (1970) and Stecher (1970) confirmed the results. Recently, Bless and Savage (1972) obtained the ultra-violet interstellar reddening curve for several stars (ζ Oph O9.5V, β^1 Sco B0.5V, $\theta^{1,2}$ Ori O8.5, σ Sco B1III, and etc.) at wavelengths extended to $1/\lambda \simeq 9.1\ \mu^{-1}$. It is found by these observations that the positions of the wavelengths of maximum interstellar absorption around $1/\lambda \simeq 4.6\ \mu^{-1}$ and the features of the reddening curves at the ultra-violet wavelengths are quite different from star to star.

Wickramasinghe and Nandy (1970, 1971a, 1971b) found that graphite-iron-silicate grain mixtures provide good fits to the observed interstellar extinction curve including the characteristic graphite feature at $1/\lambda - 4.4\ \mu^{-1}$ if one ignores the variation of the absorptivity of the silicate in the ultraviolet. Mixtures of enstatite silicate grains ($(MgFe)SiO_4$) with three types of size distribution (Huffman and Stapp, 1971) and mixtures of graphite-silicate-silicon carbide grains (Gilra, 1971) are also shown to provide good fits to the observed curves. The Gilra paper assumes constant indices of refraction for all but the graphite and therefore its predictions in the far ultraviolet are misleading. With this *basic* reservation it is explained by these grain mixtures that

* Detailed discussions of these problems will be given in *Pub. Astron. Soc. Japan* **25**, No. 2, 1973.

Greenberg and Van de Hulst (eds.), Interstellar Dust and Related Topics, 11–19.

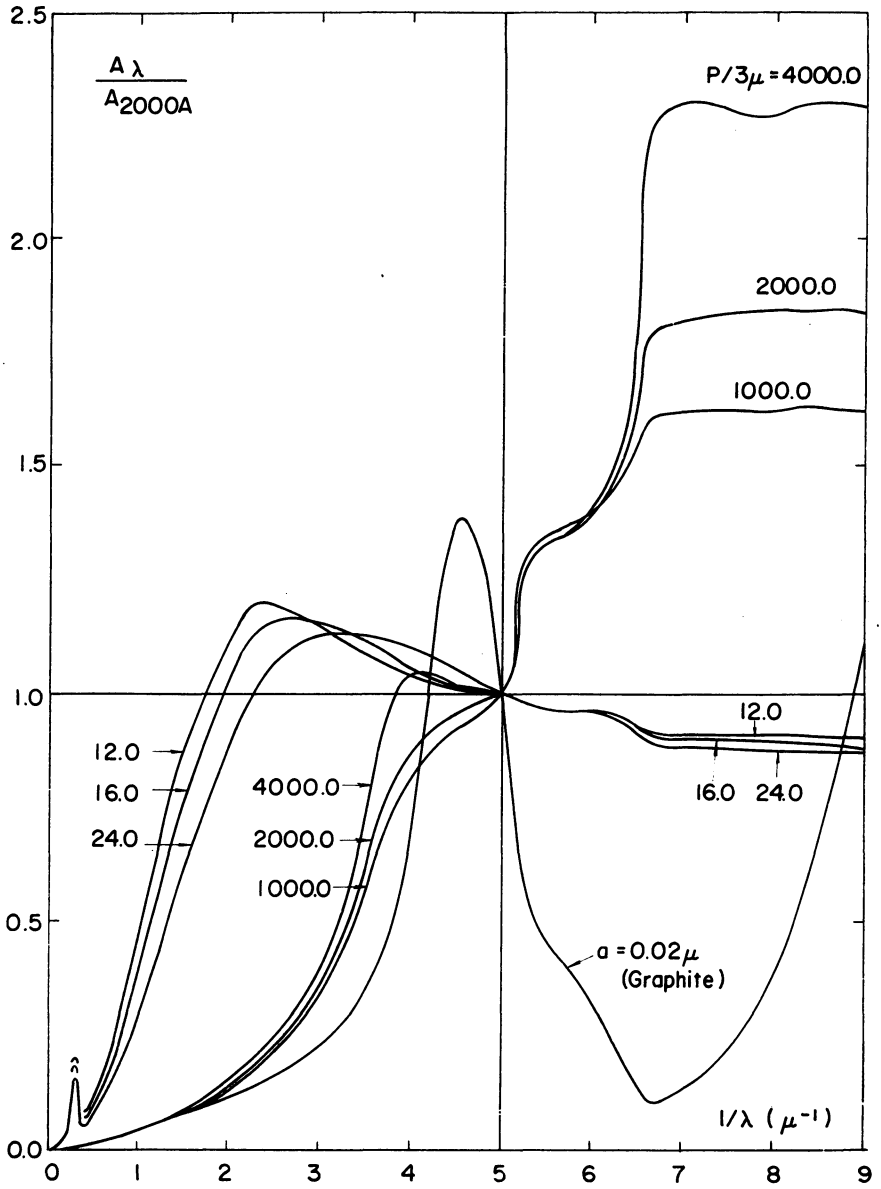

Fig. 1. The normalized extinction curves of graphite grains and graphite core-ice mantle grains. They are normalized so that the extinction at the wavelength, 2000 Å, is 1.0 mag. The size distribution of the graphite core ice mantle grains is given by $n(a) = n(0) \exp(-P/3\mu a^3)$.

the varieties of the reddening curves at the ultra-violet wavelengths may be fitted by adjusting the abundance ratio, and or, the size distribution of each grain. However, every type of grain shown in the previous papers is stable in the interstellar space and therefore the varieties of the abundance ratio and the size distribution must be made before the grains are ejected from stars.

https://doi.org/10.1017/S0074180900053973 Published online by Cambridge University Press

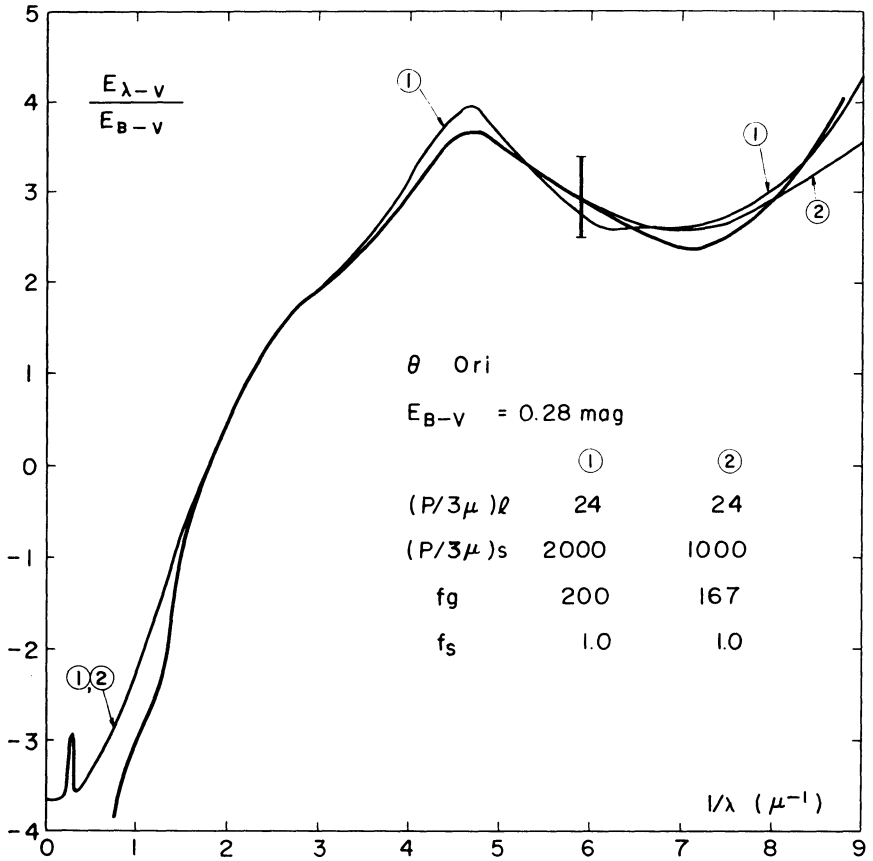

Fig. 2a. The observed and calculated extinction curves for the star $\theta^{1,2}$ Ori. The normalization is made by $A_v = 0.0$ magnitude and $E_{B-V} = 1.0$ mag. Thick line shows the observed one and thin lines show the calculated ones. The parameters of grains are shown. The vertical bar is the magnitude of the observational error.

In order to provide good fits to the observed interstellar extinction curve, we need grain mixtures with three or more types of grains and or size distributions, each one of which contributes to the extinction at the optical wavelengths, at the ultra-violet wavelength, and around $1/\lambda - 4.6\ \mu^{-1}$. Figure 1 shows the extinction curve of graphite grains with radius, 0.02 μ, and the graphite core-ice mantle grains, which are normalized so that the extinction at the wavelength, 2000 Å, is 1.0 mag. The size distribution of grains is given by $n(a) = n\,(0) \exp(-P/3\mu\, a^3)$, where P and μ are the destruction probability and the growth rate of ice mantle, respectively (Greenberg, 1966).

The graphite core-ice mantle grains with relatively large mean grain radius ($P/3\mu - 12-24$) mainly contribute to the extinction at optical and infra-red wavelengths and those with relatively small mean radius ($P/3\mu - 1000-4000$) mainly contribute to that at the ultraviolet wavelengths including the ultraviolet absorption by ice. Figures 2a and 2b show the normalized extinction curves observed by Bless and Savage (1972)

https://doi.org/10.1017/S0074180900053973 Published online by Cambridge University Press

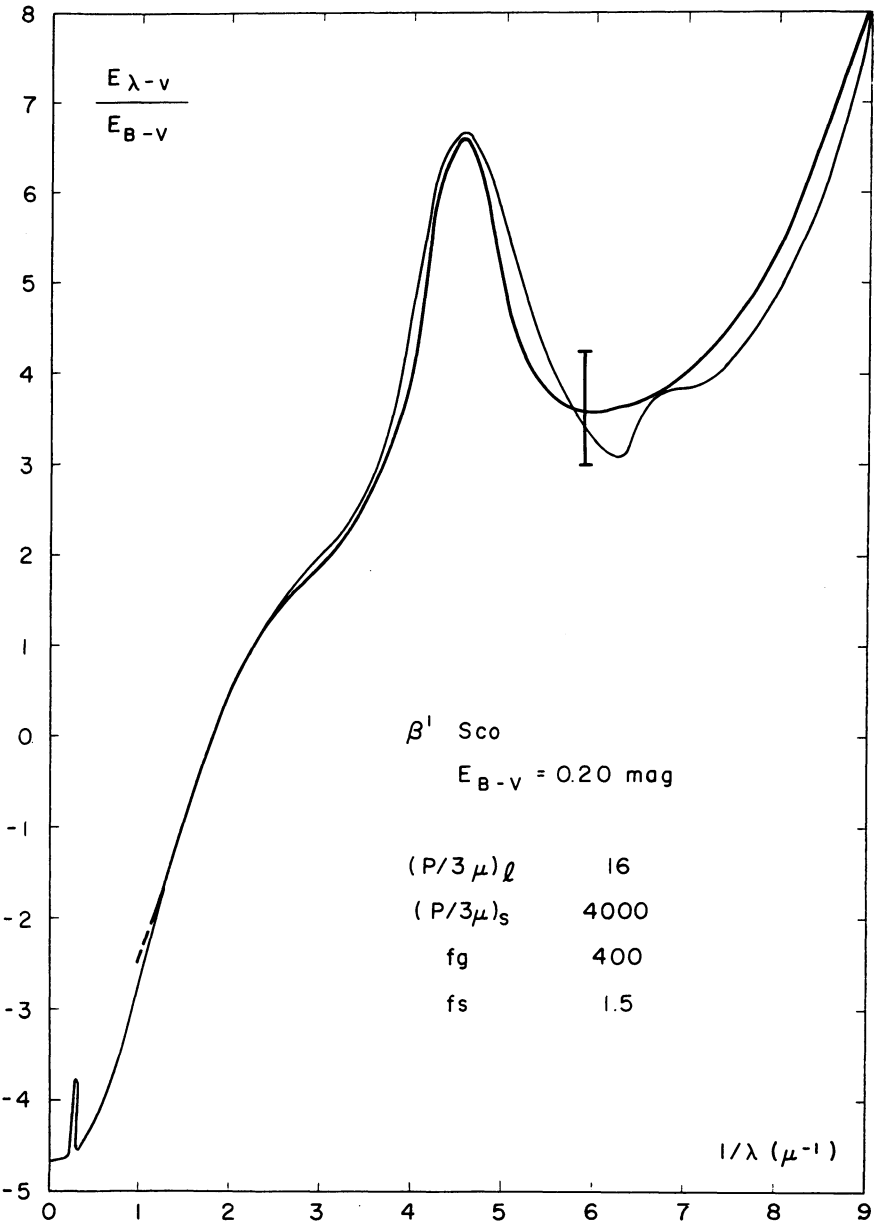

Fig. 2b. Same figure as Figure 2a, but for the star β^1 Sco.

and calculated by the author for $\theta^{1,2}$ Ori and β^2 Sco respectively. And Figures 3a and 3b show the contribution of each type of grains to the interstellar absorption. The same figures for the other stars as shown in Figure 2 are shown by Isobe (1973) and the parameters of the size distributions and the abundances of each grain are shown

https://doi.org/10.1017/S0074180900053973 Published online by Cambridge University Press

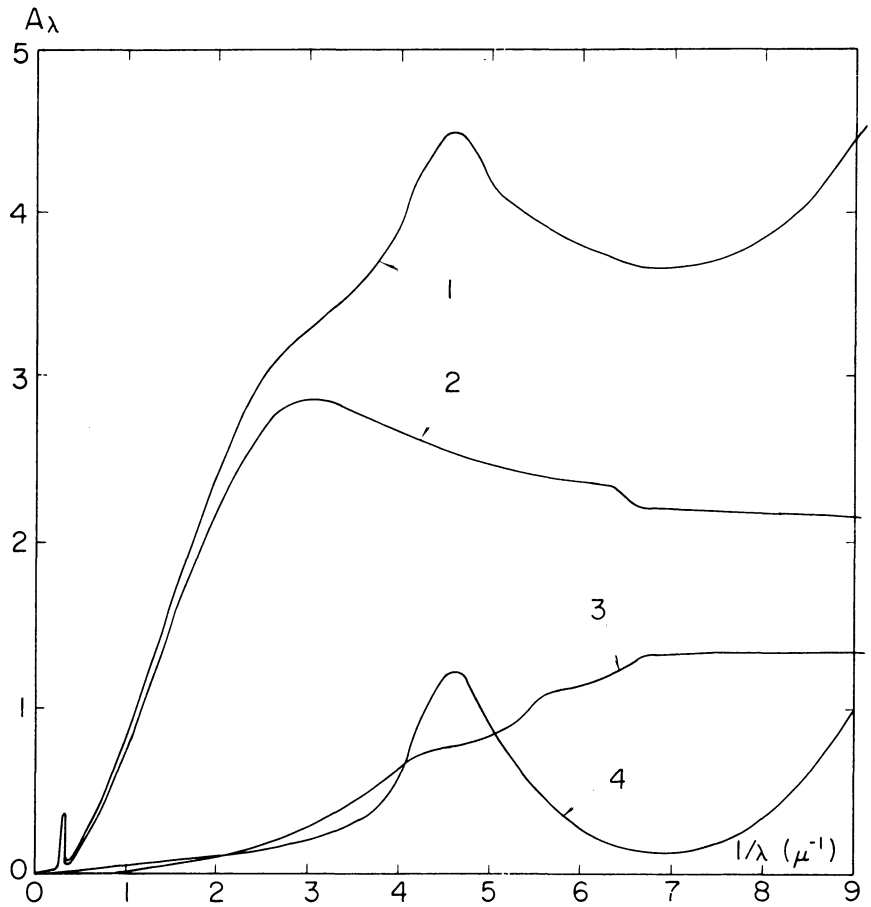

Fig. 3a. The contribution of each type of grains to the total extinction on the line of sight to $\theta^{1,2}$ Ori. The curves 2 and 3 show the extinction curves of the graphite core-ice mantle grains with large and small mean radius, respectively, and the curve 4 shows that of the graphite grains with radius of 0.02 μ. All curves are normalized so that A_v for the curve 2 is 2.0 mag. The curve 1 shows the total extinction curve.

TABLE I

Parameter of grains

	ζ Oph	σ Sco	θ Ori	β^1 Sco	Average
$(P/3\mu)_l$	24	24	24	16	20
$(P/3\mu)_s$	2000	1000	1000	4000	1000
f_g	300	300	167	400	333
f_s	3.0	1.0	1.0	1.5	2.0
$(n_d)_l$	2.8×10^{-13}	2.8×10^{-13}	2.8×10^{-13}	1.9×10^{-13}	2.3×10^{-13}
$(n_d)_s$	8.0×10^{-12}	9.9×10^{-13}	9.9×10^{-13}	1.1×10^{-11}	2.0×10^{-12}
$(n_d)_g$	2.8×10^{-11}	2.8×10^{-11}	1.8×10^{-11}	2.6×10^{-11}	2.7×10^{-11}
$(A_v)_-$	$0.^m32$	$0.^m10$	$0.^m10$	$0.^m18$	$0.^m20$

https://doi.org/10.1017/S0074180900053973 Published online by Cambridge University Press

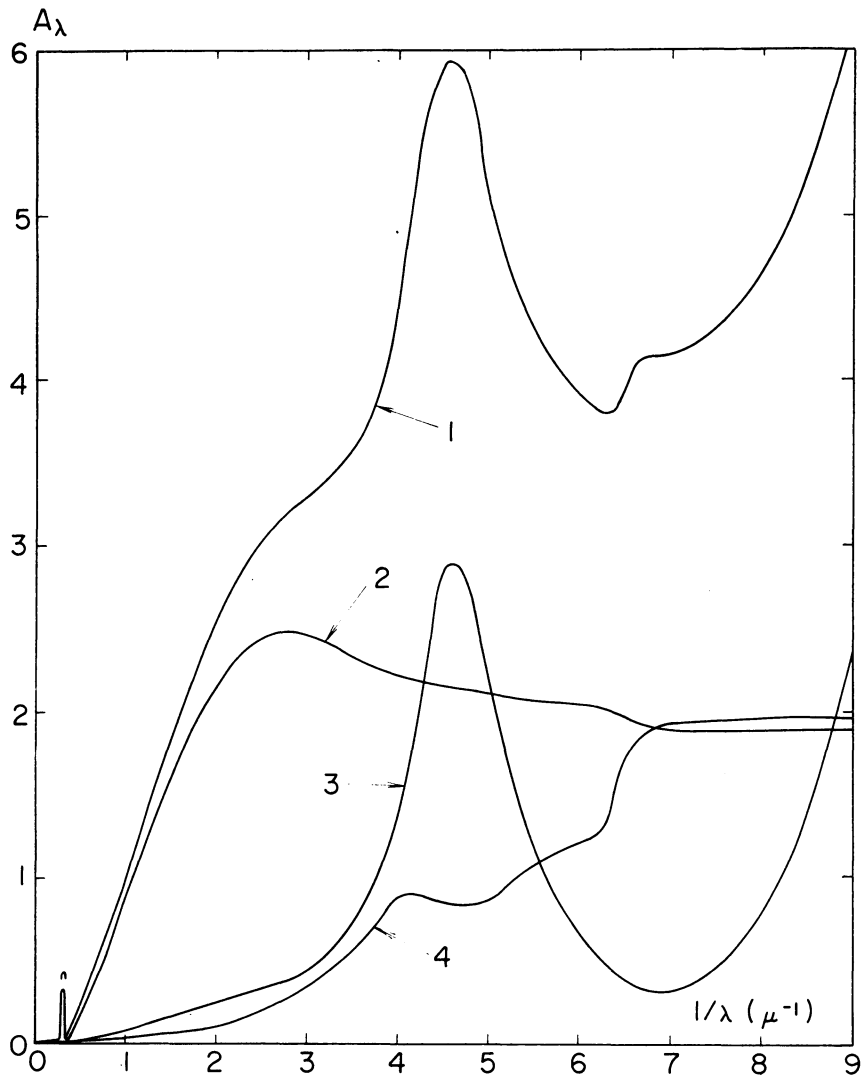

Fig. 3b. Same figure as Figure 3a, but for the case of β^1 Sco.

TABLE II

Maximum radius of grain

n_e/n_H	a_{max}
7.7×10^{-10}	0.02 μ
7.7×10^{-11}	0.04 μ
7.7×10^{-12}	0.09 μ
7.7×10^{-13}	0.20 μ
7.7×10^{-14}	0.44 μ

https://doi.org/10.1017/S0074180900053973 Published online by Cambridge University Press

TABLE III

The mean number density of interstellar grains

$P/3\mu$	n_a [a]	n_b [b]
10	8.45×10^{-14} cm^{-3}	1.19×10^{-13} cm^{-3}
20	1.61×10^{-13} cm^{-3}	2.34×10^{-13} cm^{-3}
40	2.47×10^{-13} cm^{-3}	3.47×10^{-13} cm^{-3}
60	3.75×10^{-13} cm^{-3}	6.57×10^{-13} cm^{-3}
80	7.55×10^{-13} cm^{-3}	8.91×10^{-13} cm^{-3}
100	9.91×10^{-13} cm^{-3}	1.10×10^{-12} cm^{-3}
200	2.39×10^{-12} cm^{-3}	2.21×10^{-12} cm^{-3}
400	5.95×10^{-12} cm^{-3}	4.03×10^{-12} cm^{-3}
600	1.02×10^{-11} cm^{-3}	5.84×10^{-12} cm^{-3}
800	1.50×10^{-11} cm^{-3}	7.55×10^{-12} cm^{-3}
1000	2.02×10^{-11} cm^{-3}	9.20×10^{-12} cm^{-3}
2000	5.01×10^{-11} cm^{-3}	1.68×10^{-11} cm^{-3}
4000	1.20×10^{-10} cm^{-3}	3.00×10^{-11} cm^{-3}

[a] The mean number density, when the interstellar absorption is 2.0 mag. kpc^{-1}.

[b] The mean number density, when the mean density of hydrogen atoms is 0.7 cm^{-3} in interstellar space.

in Table I. As shown in Figure 2, the observed normalized extinction curves fit well to the calculated normalized extinction curve.

It is shown by Isobe (1971) that the growth rate of ice grains is proportional to the number density of oxygen atoms in the interstellar space. However, the maximum size of ice grains in the interstellar space depends on the ratio of the number density of grains, n_g, to that of oxygen atoms, n_O, by the exhaustion of the adsorbed oxygen atoms. Table II shows the relations between the ratio, n_g/n_H, and the maximum grain radius when the ratio, n_O/n_H, is 6.76×10^{-4} (Allen, 1963, p. 30). Giving the distribution function for grain radius, $n(a) = n(0)\exp(-P/3\mu a^3)$ and considering the facts that the interstellar absorption is 2.0 mag. kpc^{-1} (Allen, 1963, p. 251), we can obtain the mean density of grains, n_a, in the interstellar space, which is shown in Table III. The mean number density, n_b, is also shown in Table III for the case that the mean number density of hydrogen atoms, n_H, is 0.7 cm^{-3} and the ratio of number density of oxygen atoms, n_O, to that of hydrogen atoms is 6.76×10^{-4} (Allen, 1963, p. 30). When $P/3\mu$ is 12–24, the number density of grain is $1.42\text{–}2.79\times10^{-13}$. The number density of graphite grains, which produce the observed 2200 Å absorption band, is f_g times of number density of the graphite core-ice mantle grains and is shown in Table I. As the gas densities in the interstellar clouds are ten times of the mean interstellar gas densities, the ratio of number density of grains to that of hydrogen is about 10^{-11}. Therefore, the ice mantle can grow up to the size of 0.09 μ, which is smaller than the mean grain of 0.2 μ in the interstellar clouds. Table IV shows the relations between the values of $P/3\mu$ and the mean grain size. However, de Jong and Kamijo (1972) show that the destruction rate of interstellar ice grains by sub-cosmic rays is independent of the grain size and is 10^{-14} cm y^{-1}, which is the same order of destruction rate as the mutual

https://doi.org/10.1017/S0074180900053973 Published online by Cambridge University Press

TABLE IV
Mean radius of grain

$P/3\mu$	$\bar{a}$	$R(=A_V/E_{B-V})$
14.6	0.22 μ	6.4
23.2	0.19 μ	4.1
40.0	0.16 μ	2.9
78.2	0.13 μ	2.2
185	0.10 μ	1.9
625	0.07 μ	1.6

impacts of grains with radius of 0.1 μ at the cloud-cloud encounters. Therefore, the adsorbed oxygen atoms are supplied to interstellar space and the ice mantle can grow up to 0.2 μ or more. From these results it follows that the interstellar reddening curves at the optical wavelengths are nearly the same in all regions of interstellar space.

If the number density of gas atoms is 0.2 times the mean interstellar gas density in the inter-cloud regions, the values of $P/3\mu$ are about 1500, which is consistent with the values of $P/3\mu$ for the grains with relatively small mean radius shown in Table I. In Table I are also shown the visual interstellar absorption by the small graphite core-ice mantle grains if the absorption by the large grains is 2.0 mag. The small grains hardly contribute to the visual absorption. In the inter-cloud regions, only 5% of interstellar atoms condense to the grains, which means that most of the atoms remain in the gas phase.

If we can somehow rationalize the assumptions regarding the ultraviolet absorptivity of ice (Greenberg, 1968) it is possible to arrive at the following conclusions: (1) that there are relatively large grains in the interstellar clouds, (2) that there are relatively small grains in the inter-cloud regions, and (3) that there are graphite grains with a size of about 0.02 μ as the kernels of the graphite core-ice mantle grains in all regions of interstellar space. Therefore, the variety of the interstellar ultra-violet absorption depends on the effective path-length ratio of the cloud regions to the inter-cloud regions along the line of sight.

References

Allen, C. W.: 1963, *Astrophysical Quantities*, 2nd ed., Athlone Press, London.
Bless, R. C. and Savage, B. D.: 1972, *Astrophys. J.* **171**, 293.
Carruthers, G. R.: 1970, in L. Houziaux and H. E. Butler (eds.), 'Ultraviolet Stellar Spectra and Related Ground-Based Observations', *IAU Symp.* **36**, 100.
De Jong, T. and Kamijo, F.: 1973, *Astron. Astrophys.* **25**, 363.
Gilra, D. P.: 1971, *Nature* **229**, 237.
Greenberg, J. M.: 1966, in K. Lodén, L. O. Lodén and U. Simerstad (eds.), 'Spectral Classification and Multicolour Photometry', *IAU Symp.* **24**, 291.
Greenberg, J. M.: 1967, in J. M. Greenberg and T. P. Roark (eds.), 'Interstellar Grains', NASA SP-140, p. 224.
Greenberg, J. M.: 1968, *Stars and Stellar Systems* **7**, 221.
Greenberg, J. M. and Shah, G. A.: 1969, *Physica* **41**, 92.
Huffman, D. R. and Stapp, J. L.: 1971, *Nature Phys. Sci.* **229**, 45.

Isobe, S.: 1971, *Publ. Astron. Soc. Japan* **24**, 27.
Isobe, S.: 1973, *Publ. Astron. Soc. Japan* **25**, 253..
Stecher, T. P.: 1965, *Astrophys. J.* **142**, 1683.
Stecher, T. P.: 1970, in L. Houziaux and H. E. Butler (eds.), 'Ultraviolet Stellar Spectra and Related Ground-Based Observations', *IAU Symp.* **36**, 24.
Trumpler, R. J.: 1930, *Lick Obs. Bull.* **14**, 154.
Wickramasinghe, N. C. and Nandy, K.: 1970, *Nature Phys. Sci.* **227**, 51.
Wickramasinghe, N. C. and Nandy, K.: 1971a, *Nature Phys. Sci.* **230**, 16.
Wickramasinghe, N. C. and Nandy, K.: 1971b, *Monthly Notices Roy. Astron. Soc.* **153**, 205.